JACS
JOURNAL OF THE AMERICAN CHEMICAL SOCIETY
Article
pubs.acs.org/JACS

Clusters Encapsulated in Endohedral Metallofullerenes: How Strained Are They?

Qingming Deng and Alexey A. Popov*

Leibniz Institute for Solid State and Materials Research, D-01171 Dresden, Germany

Supporting Information

ABSTRACT: Endohedral clusters in metallofullerenes can vary in a broad range of geometrical parameters following the size and shape of the host carbon cage. Obviously, distortions of the cluster may increase its energy and even destabilize the whole clusterfullerene molecule. However, direct evaluation of the magnitude of cluster strain energies has not been done because of the lack of a suitable computational scheme that would allow one to decouple cluster and fullerene distortions and hence estimate individual components. In this work we offer a simple and efficient scheme to calculate cluster distortion energies in endohedral metallofullerenes (EMFs). Using this scheme, we analyze distortions in three classes of EMFs with nitride, sulfide, and carbide clusters and different metal atoms (Sc, Y, Ti).

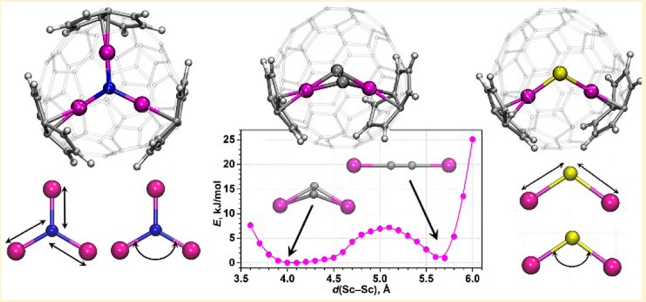

INTRODUCTION

Since the first discovery of nitride clusterfullerenes in 1999,[1] the field of clusterfullerenes, that is, endohedral metallofullerenes (EMFs) with clusters comprising both metal and nonmetal atoms, has developed dramatically.[2−6] Many types of clusters capable of being encapsulated have been discovered, including nitrides M_3N,[7,8] carbides M_2C_2,[9−11] and sulfides M_2S[12,13] (M = Sc, Y, lanthanides), to name a few. Charge transfer from the encased species to the outer framework is considered to be the main factor determining stability of the clusterfullerenes. The role of charge transfer to the carbon cage in stabilizing particular cage isomers is well-established now,[14−17] and the most preferable isomers can be routinely predicted through computation of the empty fullerene isomers in the appropriate charge states.[14,18−20]

Another important factor that also strongly influences stability of the clusterfullerenes was defined as the cage form factor.[2,17] Namely, the size and shape of the carbon cage should fit the size and shape of the encapsulated cluster. When this condition is violated, the preferable cage isomer can be switched or a given fullerene may be not formed at all. A typical example is the case of $M_3N@C_{78}$ nitride clusterfullerenes (NCFs). Whereas $D_{3h}(5)$ is preferable for relatively small Sc_3N,[21] the non-IPR (isolated pentagon rule) $C_2(22010)$ isomer is much more stable for M = Y, Dy, etc., because of the much larger size of the cluster and more suitable shape of the C_2-symmetric cage.[19] The absence of $Sc_3N@C_{72}$ and $Sc_3N@C_{74}$ in the $Sc_3N@C_{2n}$ family is also caused by the absence of suitably shaped stable isomers of C_{72} and C_{74} cages to accommodate the triangular Sc_3N cluster.[14] On the one hand, the size of the fullerene cage can also dramatically influence bond lengths or even the shape of the internal clusters. For example, a systematic experimental and computational NMR study of a series of $Y_2C_2@C_{2n}$ ($2n$ = 82, 84, 92, 100) by Dorn and co-workers[22] showed that the internal yttrium carbide cluster prefers to adopt a stretched linear shape when the cage is sufficiently large (e.g., in C_{100}), while it will bend to a compressed "butterfly shape" in relatively small cages (e.g., in C_{82}).

It is obvious that the factor of internal clusters plays a vital role in stability of clusterfullerenes, but exact energy and geometrical characteristics of encapsulated clusters are not known because in all real systems they are always templated by the carbon cage. It is therefore difficult to give a definitive answer about what an ideal structure of the internal cluster in each case should be. A computational study of the "isolated" cluster (e.g., Sc_3N) taken outside the carbon cage cannot answer the question because of the different electronic structures of free cluster and the same cluster inside the carbon cage. Electron transfer from the cluster to the cage plays an important role in their mutual stabilization. However, study of the isolated charged cluster (e.g., Sc_3N^{6+}) is also not able to give a reliable answer due to the huge Coulomb repulsion in such highly charged systems. Real charges of the endohedral cluster in EMFs are much smaller than formal ones because of the significant covalent contributions to the metal−cage interactions.[23]

In this work we offer a simple yet efficient model to overcome these problems. Coordination of metal atoms to a small organic π-system acting as a two-electron acceptor mimics the real electronic situation of the clusterfullerenes and at the

Received: December 2, 2013
Published: February 25, 2014

   dx.doi.org/10.1021/ja4122582 | J. Am. Chem. Soc. 2014, 136, 4257−4264

same time bestows on the cluster freedom to adjust its geometrical parameters in the most optimal way. We use this model to address fundamental questions about the structure and stability of three types of EMFs with M_3N, M_2S, and M_2C_2 clusters (M = Sc, Y), in particular: (i) What is an "ideal" structure of the cluster? (ii) How does the energy of each cluster change during compression, stretching, and bending?

MODEL AND COMPUTATIONAL METHODS

In nitride, sulfide, and carbide clusterfullerenes, each metal atom formally donates two electrons to the carbon cage and one electron to the non-metal bridge (N, S, and C_2, respectively). Besides, although endohedral clusters interact with the whole cage, there is a certain degree of locality in the metal–cage interactions. That is, metal atoms adjust the electron density of the "islands" of the fullerene cage, and each "island" strongly interacting with one metal atom comprises ca. 8–12 carbon atoms.[23] Hence, to mimic the electronic situation, we coordinate metal atoms to a small organic fragment capable of being a two-electron acceptor. The fragment, however, should be small enough to avoid steric hindrance when the cluster geometry is varied. The pentalene unit (two fused pentagons, C_8H_6; see Figure 1a,b) is an

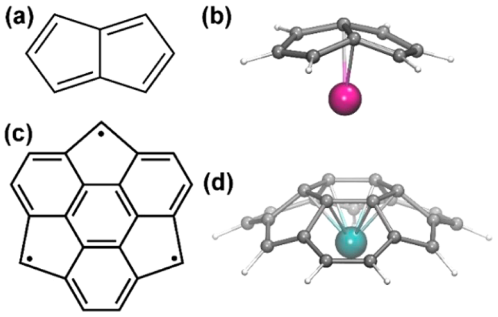

Figure 1. (a) Structural formula of pentalene C_8H_6; (b) coordination of pentalene by Sc atom (the same coordination is used for Y atoms); (c) structural formula of modified sumanene $C_{21}H_9$; (d) coordination of sumanene fragment by Ti.

ideal model system fulfilling both conditions. The use of *s*-indacene to model metal–cage interactions was also considered and gave qualitatively similar results as shown in Supporting Information. In titanium clusterfullerenes $Ti_2C_2@C_{78}$ and $Ti_2S@C_{78}$, each titanium atom donates three electrons to the cage. To model Ti–cage interactions in Ti-EMFs, we have used sumanene-like $C_{21}H_9$, which resembles a Ti-coordinated part of the carbon cage. The difference from sumanene is that only one hydrogen atom is left in each pentagon (Figure 1c). Ti is then coordinated to the central hexagon in a η^6-manner (Figure 1d).

First we optimized molecular coordinates of the clusters $M_3N(C_8H_6)_3$, $M_2S(C_8H_6)_2$, and $M_2C_2(C_8H_6)_2$ (where M = Sc or Y) and also $Ti_2S(C_{21}H_9)_2$ and $Ti_2C_2(C_{21}H_9)_2$. Then the metal–pentalene or metal–sumanene fragments were kept frozen and only internal coordinates of the cluster (i.e., angles and metal–N, metal–S, or metal–C_2 distances) were varied. When the fragments were moved too close to each other during bending or compression of the cluster so that interfragment interaction could not be ignored (the shortest interatomic distances are less than 3.0 Å), interaction energies were calculated separately and subtracted (see Supporting Information for more details).

Density functional theory (DFT) computations were carried out within a generalized gradient approximation (GGA) with PBE[24] for the exchange–correlation term, as implemented in the PRIRODA package.[25−27] Original TZ2P-quality full-electron basis sets were used as follows: {8,7,5,2}/(23s,18p,13d,7f) for Sc atoms, {6,3,2}/(11s,6p,2d) for C atoms, {6,3,2}/(11s,6p,2d) for N atoms, and {3,1}/(5s,1p) for H atoms. Stevens–Basch–Krauss (SBK)-type effective core potentials for Y and Ti atoms are treated with {5,5,4}/(9s,9p,8d) and {6,3,2}/{11s,6p,2d} valence parts. Molecular structures were visualized by use of the VMD package.[28]

RESULTS AND DISCUSSION

Nitride Clusterfullerenes. The Sc_3N cluster in the $Sc_3N(C_8H_6)_3$ molecule is a planar triangle with an optimized Sc–N bond length of 2.020 Å and a Sc–N–Sc bond angle of 120° (Figure 2a). The Sc–N bond lengths in $Sc_3N@C_{68}$,

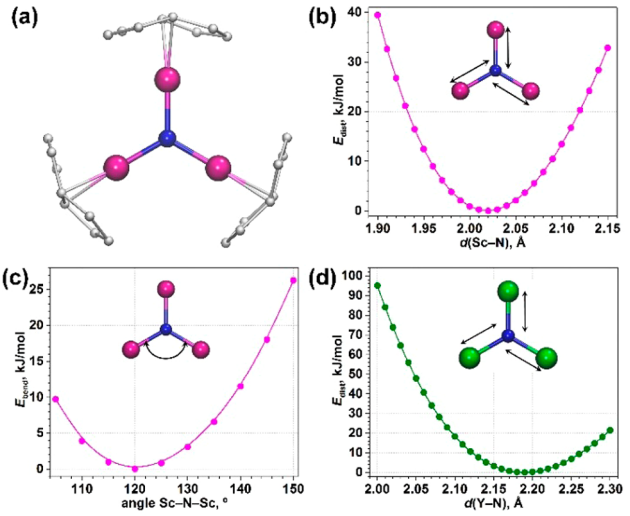

Figure 2. (a) DFT-optimized molecular structure of $Sc_3N(C_8H_6)_3$; Sc is shown in magenta, nitrogen in blue, carbon atoms in gray, and hydrogen atoms are not shown for clarity. (b–d) Energy profiles computed for (b) variation of Sc–N bond lengths in $Sc_3N(C_8H_6)_3$; (c) variation of Sc–N–Sc angle in $Sc_3N(C_8H_6)_3$; and (d) variation of Y–N bond lengths in $Y_3N(C_8H_6)_3$. In the range of computed values (110–130°), the Y–N–Y angle energy profile is identical to that for the Sc analogue.

$Sc_3N@C_{78}$, and $Sc_3N@C_{80}$ optimized at the same level of theory are 1.993, 2.010, and 2.033 Å, respectively, and the Sc–N–Sc bond angles are all 120°. Analogous variations of the Sc–N bond length in the $Sc_3N(C_8H_6)_3$ complex produced only small changes in the energy (1.8, 0.2, and 0.5 kJ·mol^{-1}, respectively). However, when the cluster in $Sc_3N(C_8H_6)_3$ was distorted in the same way as in $Sc_3N@C_{70}$ (Sc–N–Sc bond angles are 150° and 2 × 105°, whereas bond lengths are 1.988 and 2.059 Å), the energy increased dramatically to 50 kJ·mol^{-1}. This large strain value may explain the low yield of $Sc_3N@C_{70}$ in comparison to $Sc_3N@C_{68}$ and $Sc_3N@C_{78}$.[18] To get a more detailed description of the structure–energy relationships, we have computed energy profiles along Sc–N bond stretching/elongation in the 1.900–2.150 Å range (Figure 2b) and along Sc–N–Sc angle bending in the 105–150° range (Figure 2c). Corresponding distortion energies will be hereafter denoted as E_{dist} and E_{bend}. The E_{dist} energy of the $Sc_3N(C_8H_6)_3$ molecule remains within 10 kJ·mol^{-1} in the 2.02 ± 0.06 Å range of Sc–N bond lengths. Thus, the Sc_3N cluster in NCFs is rather flexible in terms of Sc–N bond lengths. The Sc–N–Sc bending profile is also rather flat within the 110–135° range (energy of the system remains below 10 kJ·mol^{-1}). For larger distortion angles, a steep increase of E_{bend} is observed.

The free $Y_3N(C_8H_6)_3$ molecule has a similar structure to $Sc_3N(C_8H_6)_3$ with the exception that the Y–N bond length is elongated to 2.190 Å. Compression of Y–N average bond lengths in $Y_3N@C_{78}$-C_2 and $Y_3N@C_{80}$ to 2.099 and 2.060 Å

dx.doi.org/10.1021/ja4122582 | J. Am. Chem. Soc. 2014, 136, 4257–4264

respectively increases the energy by 21 and 42 kJ·mol^{-1}. One Y−N−Y angle in $Y_3N@C_{78}$ is bent to 125.5°, and those in $Y_3N@C_{80}$ are slightly changed to 119.8°. Cluster distortion energy in hypothetical $Y_3N@C_{78}$-$D_{3h}(5)$ (i.e., with the same carbon cage as $Sc_3N@C_{78}$) is as high as 72 kJ·mol^{-1}. In $Y_3N@C_{82}$, the average Y−N length became 2.131 Å, resulting in distortion energy of 14 kJ·mol^{-1}. With further increase of cage size, the average Y−N bond length increases to 2.162 Å in $Y_3N@C_{84}$, 2.173 Å in $Y_3N@C_{86}$, and 2.194 Å in $Y_3N@C_{88}$, whereas the angles deviate from 120° by no more than by 10°. With these geometrical parameters, distortion energies of the $Y_3N(C_8H_6)_3$ molecule are 2, 5, and 1 kJ·mol^{-1}, respectively.

Our results show that the Y_3N cluster is significantly strained in $Y_3N@C_{80}$ and the strain is much lower in the large cages C_{82}−C_{88}. Extraordinary high stability of the $[C_{80}$-$I_h]^{6-}$ cage results in a higher yield of $Y_3N@C_{80}$-I_h in synthesis in comparison to $Y_3N@C_{2n}$ ($2n$ = 82−88), but further increase of the metal (Gd and beyond) leads to drastic decrease of the relative yield of $M_3N@C_{80}$. Besides, the yield of $Y_3N@C_{80}$ is much lower than that of $Sc_3N@C_{80}$ (the cluster is not strained in the latter), and high strain of the nitride cluster is presumably one of the reasons.

The energy profile along Y−N bond length variation (Figure 2d) shows that the optimal bond length for $Y_3N(C_8H_6)_3$ is about 2.19 ± 0.07 Å, which is 0.17 Å longer than the Sc−N bond length. Variation of Y−N−Y angles from 110° to 130° (the range of experimentally known clusterfullerenes) has a small effect on the energy. These data clearly show that cages larger than C_{82} are preferable for the Y_3N cluster and that E_{dist} is the main component in cluster distortion energies of the $Y_3N@C_{2n}$ molecules.

Sulfide Clusterfullerenes. Since its discovery in 2010,[6] the family of sulfide clusterfullerenes, $Sc_2S@C_{2n}$, has expanded to four members with cage sizes from C_{70} to C_{82}.[20,29,30] Analysis of geometrical parameters of the Sc_2S cluster in these molecules reveals that the Sc_2S unit is very flexible and can adopt substantially different Sc−S−Sc bond angles in different cages (Figure 3). In the X-ray-characterized isomers of $Sc_2S@C_{82}$, the Sc_2S cluster is bent with Sc−S−Sc angles of 114° and 97° in $C_s(6)$ and $C_{3v}(8)$ cages, respectively.[30] DFT studies of $Sc_2S@C_{70}$-$C_2(7892)$[20] and $Sc_2S@C_{72}$-$C_s(10528)$[29] also predict bent cluster with angles of 98° and 124°, respectively, whereas computational study of $Sc_2S@C_{74}$-$C_2(13333)$ shows that in this cage the Sc_2S cluster can be linear (note that this structure has not been isolated so far). The questions thus appear to be (i) what the optimal shape of the sulfide cluster is and (ii) how sensitive the stability of the sulfide clusterfullerene is to deformation of the cluster.

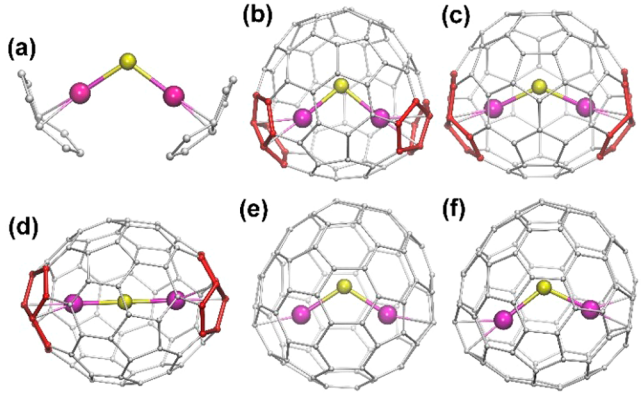

Figure 3. DFT-optimized structures of (a) $Sc_2S(C_8H_6)_2$ and (b−f) Sc−sulfide clusterfullerenes: (b) $Sc_2S@C_{70}$-$C_2(7892)$, (c) $Sc_2S@C_{72}$-$C_s(10528)$, (d) $Sc_2S@C_{74}$-$C_2(13333)$, (e) $Sc_2S@C_{82}$-$C_{3v}(8)$, and (f) $Sc_2S@C_{82}$-$C_s(6)$.

Unconstrained optimization of the $Sc_2S(C_8H_6)_2$ molecule resulted in a bent Sc_2S cluster with bond length of 2.411 Å and Sc−S−Sc angle of 110° (Figure 3a). Distortion energies computed for the cluster in experimentally available cages were 16 kJ·mol^{-1} for $Sc_2S@C_{70}$ and <10 kJ/mol for all other cages (Table 1).

Similar to Sc_3N, the Sc_2S cluster is rather flexible in terms of metal−sulfur bond length. E_{dist} remains below 10 kJ/mol when the Sc−S distance is varied in the 2.32−2.50 Å range (i.e., ±0.09 Å from the optimal value), and only at distances shorter than 2.32 Å is the 10 kJ·mol^{-1} threshold overcome (Figure 4a). Variation of the Sc−S−Sc angle from 95° to 180° also does not lead to strong destabilization of the structure. The optimal angle is about 110°, but it can vary within rather large limits with modest energy increase (Figure 4b). The linear structure corresponds to the energy maximum with E_{bend} = 6 kJ·mol^{-1}, and similarly small energy changes are found when the Sc−S−Sc angle is decreased from 110° to 95° (at angles below 95°, the pentalene fragments start to interact strongly, which makes the values nonreliable). Thus, our calculations show that the Sc_2S cluster can adopt the shape dictated by the carbon cage without a pronounced increase in energy, which agrees with the variety of geometric parameters of the Sc_2S cluster found in clusterfullerenes.

For larger metal atoms (e.g., Y), only the $M_2S@C_{82}$ structures have been observed so far,[12] but dedicated studies of such sulfides have not been performed yet. Optimization of the $Y_2S(C_8H_6)_2$ molecule yields a bond length of 2.58 Å (0.17 Å longer than in Sc_2S) and a Y−S−Y angle of 140°. In all $Y_2S@C_{2n}$ clusterfullerenes studied in this work (Table 1), the cluster is significantly strained, with distortion energies from 26 kJ·mol^{-1} in $Y_2S@C_{82}$-$C_{3v}(8)$ to 53 kJ·mol^{-1} in $Y_2S@C_{70}$-$C_2(7892)$. The Y−S−Y angles in EMFs (86−105°) are all much smaller than in $Y_2S(C_8H_6)_2$, and the Y−S bonds (2.46−2.49 Å) are all noticeably shorter than the optimal value.

The energy profile computed along Y−S bond length shows that distortion energy remains below 10 kJ·mol^{-1} when the bond length deviates from the optimal value of 2.58 Å within a ±0.10 Å interval (Figure 4c). However, Y−S distances in $Y_2S@C_{2n}$ molecules are shorter, resulting in E_{dist} contributions to distortion energies of 8−16 kJ·mol^{-1}. The E_{bend} profile shows that the Y_2S cluster is very flexible in the range 125−180° (energy is below 1 kJ/mol; see Figure 4d). At smaller angles the energy rise is relatively steep, reaching 8 kJ·mol^{-1} at 105° (as in $Y_2S@C_{72}$), 14 kJ·mol^{-1} at 97° ($Y_2S@C_{82}$), and 31 kJ·mol^{-1} at 86° ($Y_2S@C_{70}$). Thus, we can conclude that the Y_2S cluster is noticeably strained in C_{70}, C_{72}, and C_{82} cages. In $Y_2S@C_{72}$ and $Y_2S@C_{82}$, both compression of the cluster (E_{dist}) and its bending have comparable contributions to the distortion energy, whereas in $Y_2S@C_{70}$, E_{bend} is twice the value of E_{dist}. $Y_2S@C_{2n}$ with larger cages have not been considered in this work, but from E_{dist} and E_{bend} profiles we can conclude that distortion energies in such sulfide clusterfullerenes will be small, and hence these molecules can be viable synthetic targets similar to already-known carbide clusterfullerenes.

Carbide Clusterfullerenes. Structural analysis of carbide clusters M_2C_2 (M = Sc, Y) is more complex than for M_3N and M_2S because the C_2 unit can rotate and adopt different

dx.doi.org/10.1021/ja4122582 | J. Am. Chem. Soc. 2014, 136, 4257−4264

Table 1. Distortion Energies and Cluster Geometry Parameters in Selected Nitride and Sulfide Clusterfullerenes[a]

EMF molecule	E, kJ·mol^{-1}	E_{dist}, kJ·mol^{-1}	E_{bend}, kJ·mol^{-1}	d(M−X), Å	α(M−X−M), deg
			Nitride Clusterfullerenes		
$Sc_3N(C_8H_6)_3$	0.0	0.0	0.0	2.020	120.0
$Sc_3N@C_{68}$-D_3(6140)	1.8	1.7	0.0	1.993	120.0
$Sc_3N@C_{70}$-C_{2v}(7854)	49.6	0.1	47.1	1.988, 2.059	2 × 105.0, 150.0
$Sc_3N@C_{78}$-D_{3h}(5)	0.2	0.2	0.0	2.010	120.0
$Sc_3N@C_{80}$-I_h(7)	0.5	0.4	0.0	3.033	120.0
$Y_3N(C_8H_6)_3$	0.0	0.0	0.0	2.190	120.0
$Y_3N@C_{78}$-D_{3h}(5)	72.3	30.5	30.3	2.076	113.2
$Y_3N@C_{78}$-C_2(22010)	21.1	18.8	1.0	2.100	117.2−125.5
$Y_3N@C_{80}$-I_h(7)	41.5	50.7	0.5	2.060	119.9
$Y_3N@C_{82}$-C_s(39663)	13.8	7.5	4.8	2.131	113.5−131.0
$Y_3N@C_{84}$-C_s(51365)	5.4	2.3	2.5	2.156	113.5−125.9
$Y_3N@C_{86}$-D_3(19)	2.2	0.6	1.5	2.173	119.9
$Y_3N@C_{88}$-D_2(35)	1.2	0.1	1.2	2.195	117.6−124.9
			Sulfide Clusterfullerenes		
$Sc_2S(C_8H_6)_2$	0.0	0.0	0.0	2.411	110.3
$Sc_2S@C_{70}$-C_2(7892)	16.0	2.4	10.4	2.363	97.6
$Sc_2S@C_{72}$-C_s(10528)	5.2	3.4	2.2	2.354	127.5
$Sc_2S@C_{74}$-C_2(13333)	9.0	3.4	6.1	2.354	175.8
$Sc_2S@C_{82}$-C_{3v}(8)	2.0	2.1	0.2	2.366	113.6
$Sc_2S@C_{82}$-C_s(6)	1.8	1.6	0.3	2.373	114.6
$Y_2S(C_8H_6)_2$	0.0	0.0	0.0	2.578	140.4
$Y_2S@C_{70}$-C_2(7892)	53.4	11.3	30.9	2.474	86.4
$Y_2S@C_{72}$-C_s(10528)	28.4	15.9	7.7	2.456	104.7
$Y_2S@C_{82}$-C_{3v}(8)	25.8	8.7	14.0	2.486	97.2

[a]X is either N or S; M is either Sc or Y. All parameters are for DFT-optimized structures. Distortion energies listed in the table are computed for model molecules [such as $Sc_3N(C_8H_6)_3$] whose geometrical parameters were adjusted to be identical to the cluster geometry in corresponding EMFs.

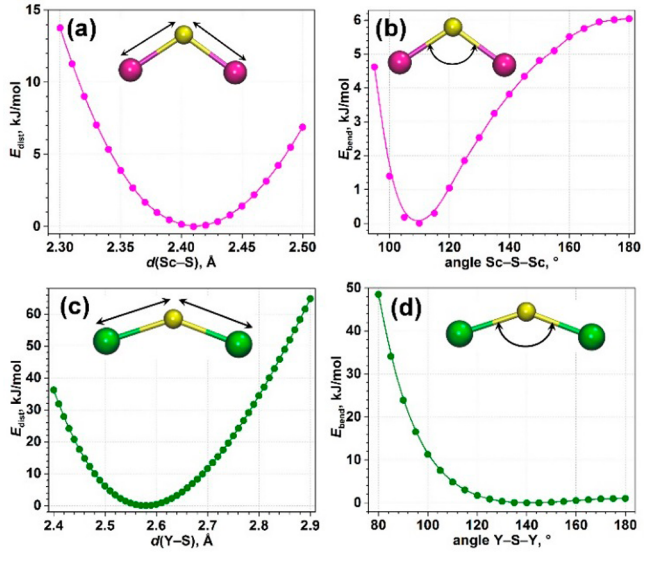

Figure 4. Energy profiles computed for (a) variation of Sc−S bond length in $Sc_2S(C_8H_6)_2$, (b) variation of Sc−S−Sc angle in $Sc_2S(C_8H_6)_2$, (c) variation of Y−S bond length in $Y_2S(C_8H_6)_2$, and (b) variation of Y−S−Y angle in $Y_2S(C_8H_6)_2$.

orientations with respect to metal atoms depending on the carbon cage (Figure 5).[22,31] For instance, Krause et al.[32] reported that the C_2 unit of $Sc_2C_2@C_{84}$ is perpendicular to two Sc atoms, which are located on the S_4 axis of the C_{84}-D_{2d} cage. In the X-ray structure of $Sc_2C_2@C_{82}$, the cluster has a butterfly shape with an average angle between two Sc−C−C planes of 130°.[31] In a recent study, Dorn and co-workers[22] reported that Y_2C_2 cluster is gradually changing its geometry from a stretched linear chain in $Y_2C_2@C_{100}$ to a compressed butterfly shape in $Y_2C_2@C_{82}$. The authors interpreted these changes as a manifestation of the "nanoscale fullerene compression".

Sc−Carbide Clusters. The lowest-energy structure of $Sc_2C_2(C_8H_6)_2$ has a butterfly shape as shown in Figure 5a. The Sc−Sc distance is 4.044 Å, and the C_2 carbide unit is perpendicular to a line between the two metal atoms. The angle between two Sc−C−C planes (which is equal to the Sc−C−C−Sc dihedral angle) is 129°. This cluster shape closely resembles that found in $Sc_2C_2@C_{82}$-C_{3v}(8). However, we have found that $Sc_2C_2(C_8H_6)_2$ with linear Sc−C−C−Sc cluster and Sc−Sc distance of 5.656 Å (Figure 5b) is also an energy minimum and is only 1 kJ·mol^{-1} higher in energy than the butterfly-shaped configuration. We therefore decided to analyze how the energy of the system is changing in dependence on the Sc···Sc separation. Figure 6a shows the energy profile obtained by fixing Sc atoms at different distances and allowing the C_2 unit to relax. The energy remains below 10 kJ·mol^{-1} over a broad range of Sc···Sc distances, proving that Sc_2C_2 cluster is also rather flexible. Shortening the distance between metal atoms leads to a decrease in the Sc−C−C−Sc dihedral angle from 129° at the energy minimum of 4.044 Å to 109° at 3.600 Å. Decrease of the dihedral angle is accompanied by a gradual shortening of Sc−C bond lengths (from 2.33 to 2.30 Å). These structural changes lead to moderate energy increase: at the shortest studied distance of 3.6 Å, the energy is increased to 7.6 kJ·mol^{-1}.

The increase in Sc···Sc distance beyond 4.04 Å first results in flattening of the Sc_2C_2 cluster (decrease of the Sc−C−C−Sc dihedral angle), which adopts a planar shape at 4.5 Å. The Sc−

dx.doi.org/10.1021/ja4122582 | J. Am. Chem. Soc. 2014, 136, 4257−4264

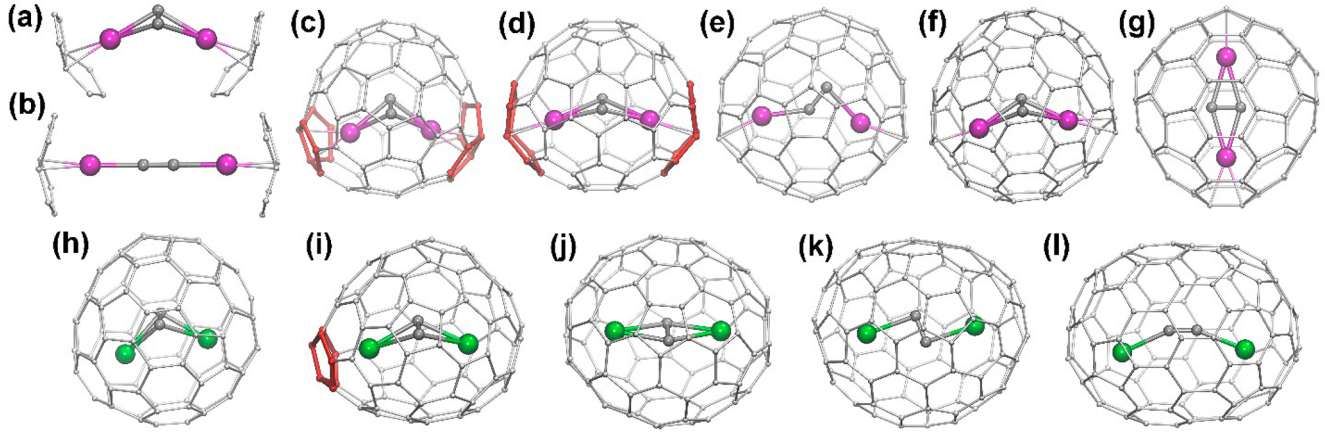

Figure 5. (a) Butterfly and (b) linear configurations of the Sc_2C_2 cluster in $Sc_2C_2(C_8H_6)_2$. (c–g) DFT-optimized structures of Sc–carbide clusterfullerenes: (c) Sc_2C_2@C_{70}-C_2(7892), (d) Sc_2C_2@C_{72}-C_s(10528), (e) Sc_2C_2@C_{80}-C_{2v}(5), (f) Sc_2C_2@C_{82}-C_{3v}(8), and (g) Sc_2C_2@C_{84}-D_{2d}(23). (h–l) DFT-optimized structures of Y–carbide clusterfullerenes: (h) Y_2C_2@C_{82}-C_{3v}(8), (i) Y_2C_2@C_{84}-C_1(51383), (j) Y_2C_2@C_{88}-D_2(35), (k) Y_2C_2@C_{92}-D_3(85), and (l) Y_2C_2@C_{100}-D_5(450). Sc atoms are shown in magenta, Y atoms in green, and carbon atoms in gray or red (in adjacent pentagon pairs). Hydrogen atoms in panels a and b are omitted for clarity.

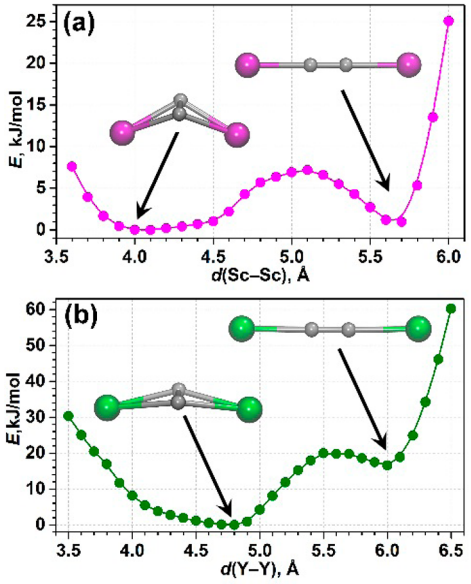

Figure 6. Energy profiles computed for (a) variation of Sc–Sc distance in $Sc_2C_2(C_8H_6)_2$; and (b) variation of Y–Y distance in $Y_2C_2(C_8H_6)_2$. Energy minima corresponding to butterfly and linear configurations of M_2C_2 clusters are pointed by arrows.

C distances remain near 2.33 Å in the whole 4.0–4.5 Å range, and the C_2 unit remains perpendicular to the Sc–Sc line. Further separation of Sc atoms leaves the cluster planar, but the C_2 unit starts to rotate in the cluster plane till it reaches a linear Sc–C–C–Sc configuration at 5.656 Å. Transformation from a perpendicular shape to a linear one requires an energy barrier of 7.2 kJ·mol^{-1}, which is reached at the Sc···Sc distance of 5.1 Å. Note that the center of the C_2 unit does not remain on the Sc–Sc line during rotation of the group. Besides, as the C_2 group starts to rotate, the two Sc–C distances for each Sc atom become nonequivalent. The shortest one remains almost constant (2.18–2.19 Å) when the Sc···Sc distance is varied in the range of 4.8–5.6 Å; that is, till the cluster adopts a linear shape. Further increase of the Sc···Sc distance results in increased Sc–C bond length and rapid increase of the energy. During the whole scan of Sc···Sc distances, the C_2 unit remains very rigid: the shortest and longest C≡C bond lengths found are 1.252 and 1.272 Å.

Table 2 lists cluster distortion energies computed for five Sc-based carbide clusterfullerenes: Sc_2C_2@C_{70}-C_2(7892), Sc_2C_2@C_{72}-C_s(10528),[33] Sc_2C_2@C_{80}-C_{2v}(5),[34] Sc_2C_2@C_{82}-C_{3v}(8),[35] and Sc_2C_2@C_{84}-D_{2d}(23).[9] Sc_2C_2@C_{70} has not been characterized yet but was studied here as an analogous structure to Sc_2S@C_{70}. The Sc···Sc distance in these molecules varies from 3.587 Å in Sc_2C_2@C_{70} to 4.451 Å in Sc_2C_2@C_{84}. These values correspond to the range of the butterfly-shaped Sc_2C_2 found in calculations for $Sc_2C_2(C_8H_6)_2$, and four of five carbide clusterfullerene molecules indeed have such a shape. The outlier is Sc_2C_2@C_{80}: the shape of its cluster resembles that of

Table 2. Distortion Energies and Cluster Geometry Parameters in Selected Carbide Clusterfullerenes[a]

EMF molecule	E, kJ·mol^{-1}	M–M, Å	C≡C, Å	M–C–C–M, deg
Sc–Carbide Clusters				
$Sc_2C_2(C_8H_6)_2$-butterfly	0.0	4.044	1.271	129.0
$Sc_2C_2(C_8H_6)_2$-linear	1.0	5.656	1.256	179.5
Sc_2C_2@C_{70}-C_2(7892)	20.5	3.587	1.263	108.5
Sc_2C_2@C_{72}-C_s(10528)	8.9	4.230	1.265	149.0
Sc_2C_2@C_{80}-C_{2v}(5)	14.8	4.390	1.258	179.8
Sc_2C_2@C_{82}-C_{3v}(8)	1.9	3.966	1.271	129.1
Sc_2C_2@C_{84}-D_{2d}(23)	1.6	4.451	1.274	180.0
Y–Carbide Clusters				
$Y_2C_2(C_8H_6)_2$-butterfly	0.0	4.809	1.270	167.5
$Y_2C_2(C_8H_6)_2$-linear	16.0	5.991	1.254	173.7
Y_2C_2@C_{82}-C_{3v}(8)	25.0	3.793	1.267	109.7
Y_2C_2@C_{84}-C_1(51383)	9.4	4.257	1.266	131.5
Y_2C_2@C_{88}-D_2(35)	9.5	4.642	1.267	177.8
Y_2C_2@C_{92}-D_3(85)	5.5	4.880	1.266	176.0
Y_2C_2@C_{100}-D_5(450)	27.4	5.516	1.252	169.0

[a]All parameters are for DFT-optimized structures. Distortion energies listed in the table are computed for model molecules [such as $Sc_2C_2(C_8H_6)_2$] whose geometrical parameters were adjusted to be identical to the cluster geometry in corresponding EMFs.

dx.doi.org/10.1021/ja4122582 | J. Am. Chem. Soc. 2014, 136, 4257–4264

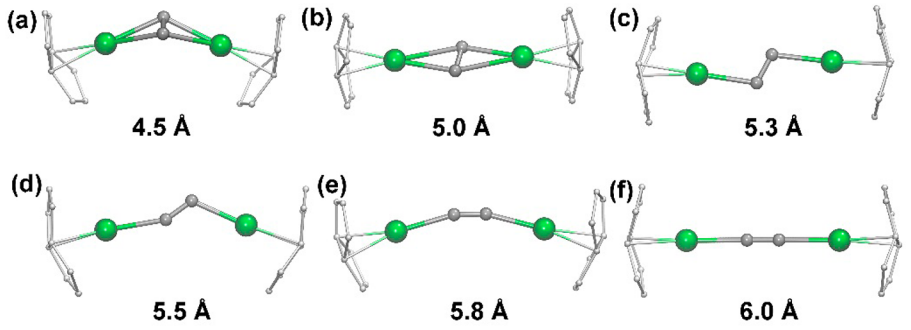

Figure 7. Evolution of $Y_2C_2(C_8H_6)_2$ molecular structure with increasing Y···Y distance from 4.5 to 6.0 Å. The energies are (a) 1.0, (b) 4.2, (c) 15.2, (d) 20.0, (e) 18.6, and (f) 16.6 kJ·mol^{-1}. Y atoms are shown in green and carbon atoms in gray; hydrogen atoms are omitted for clarity.

the $Sc_2C_2(C_8H_6)_2$ molecule with the Sc···Sc distance fixed at 4.8–4.9 Å; that is, the cluster is planar, the C_2 unit is rotated in the cluster plane, and its center is shifted from the Sc–Sc line. Variation of the Sc_2C_2 cluster geometry in different carbon cages was analyzed in ref 36. In $Sc_2C_2@C_{90}$ with elongated C_{90}-D_{5h} cage, the authors showed that the cluster can have almost a linear configuration.

The carbide cluster $Sc_2C_2@C_{70}$ has the shortest Sc–Sc distance (3.587 Å) and the highest distortion energy (21 kJ·mol^{-1}). The least strained clusters with distortion energies less than 2 kJ·mol^{-1} are found in $Sc_2C_2@C_{82}$ and $Sc_2C_2@C_{84}$. Distortion energies in $Sc_2C_2@C_{72}$ and $Sc_2C_2@C_{80}$ have intermediate values of 9 and 15 kJ·mol^{-1}. Note that the cluster distortion energies in $Sc_2C_2@C_{70}$, $Sc_2C_2@C_{72}$, and $Sc_2C_2@C_{80}$ are higher than might be expected from the $Sc_2C_2(C_8H_6)_2$ calculations with the same Sc···Sc distances, whereas the shape of the cluster in $Sc_2C_2@C_{80}$ (see above), and to some extent in $Sc_2C_2@C_{72}$, deviates from that in $Sc_2C_2(C_8H_6)_2$. This result shows that the way Sc atoms are coordinated to the cage fragments may also play some role in determining the shape of the cluster and its stability. However, deviations of distortion energies are still not very high and show that Sc_2C_2 is rather flexible and can adopt different configurations following the shape of the host carbon cage.

Y–Carbide Clusters. Similar to $Sc_2C_2(C_8H_6)_2$, calculations of $Y_2C_2(C_8H_6)_2$ revealed the presence of two energy minima, with butterfly-shaped and linear Y_2C_2 clusters. However, in contrast to the Sc case, these minima are not isoenergetic. The structure with butterfly-shaped Y_2C_2 cluster (Y···Y distance 4.809 Å) is 16 kJ·mol^{-1} lower in energy than the configuration with linear cluster (Y···Y distance 5.991 Å). The profile computed in the Y···Y range from 4.0 to 6.5 Å shows a very flat region at 4.0–5.1 Å, where energy remains below 10 kJ·mol^{-1} (Figure 6b). At longer Y···Y distances, the energy increases to 20 kJ·mol^{-1} (at 5.5 Å), then slowly decreases to 17 kJ/mol near 5.9–6.0 Å, and then grows fast to 62 kJ·mol^{-1} at 6.5 Å. Figure 7 shows the evolution of Y_2C_2 structure with increasing Y···Y distance.

Distortion energies computed for the Y_2C_2 cluster in experimentally available carbide clusterfullerenes $Y_2C_2@C_{82}$-$C_{3v}(8)$,[37] $Y_2C_2@C_{84}$-$C_1(51383)$,[38,39] $Y_2C_2@C_{88}$-$D_2(35)$,[40] $Y_2C_2@C_{92}$-$D_3(85)$,[22,41,42] and $Y_2C_2@C_{100}$-$D_5(450)$[22] (see Table 2) agree with the trend found in the Y···Y energy profile of $Y_2C_2(C_8H_6)_2$. The largest distortion energy, 27 kJ·mol^{-1}, is found in $Y_2C_2@C_{100}$ with the largest carbon cage and longest Y···Y distance (5.516 Å). This distance corresponds to the energy maximum of $Y_2C_2(C_8H_6)_2$ (Figure 6b). Similarly large distortion energy, 25 kJ·mol^{-1}, is also found in $Y_2C_2@C_{82}$. Here the Y···Y distance, 3.793 Å, is too short because of the small size of the cage. The least strained cluster is in $Y_2C_2@C_{92}$ (6 kJ·mol^{-1}), whereas in $Y_2C_2@C_{84}$ and $Y_2C_2@C_{88}$ the energies are higher but still do not exceed 10 kJ·mol^{-1}. The Y···Y distance for the latter three structures fall in the range from 4.257 to 4.880 Å, and the cluster adopts a butterfly shape with different Y–C–C–Y dihedral angles.

For the sake of comparison, we have also performed calculations for $[M_2C_2]^{4+}$ clusters. In agreement with earlier results,[22] for both Sc and Y we found only one energy minimum corresponding to the linear configuration of the cluster. M···M distances in these configurations are 5.794 Å for Y and 5.528 Å for Sc. At shorter metal–metal distances, the energy of $[M_2C_2]^{4+}$ clusters increases dramatically, reaching 150 kJ·mol^{-1} for $[Y_2C_2]^{4+}$ at 4.8 Å and 280 kJ·mol^{-1} for $[Sc_2C_2]^{4+}$ at 4.0 Å. In $M_2C_2(C_8H_6)_2$ calculations, these metal–metal distances correspond to the lowest-energy butterfly configurations. Thus, we believe that because of uncompensated Coulomb repulsion, the $[M_2C_2]^{4+}$ model gives the wrong description of cluster energetics at short M···M distances. Coordinating the metal atoms to pentalene fragments reduces unphysical repulsion and gives a more correct description of the cluster in EMFs.

Our results show that the background of the "nanoscale fullerene compression", which implies that the least strained structure of Y_2C_2 is linear and that the butterfly shape is forced by cage-induced compression, should be reconsidered. In fact, a butterfly shape of the M_2C_2 cluster is more energetically favorable and is realized when the metal–metal distance is ca. 4–5 Å. At shorter distances the energy is increasing, and "nanoscale compression" is really an appropriate term. However, at longer distances the energy is also increasing and the linear form is higher in energy, especially for Y_2C_2. Thus, "nanoscale stretching" would be an appropriate term for the longer metal–metal distances. In fact, the shape and the size of the carbon cage determine the position of metal atoms and the M···M distance (M–cage distances are more or less constant), whereas the C_2 unit then finds its best configuration for a given position of metal atoms.

$Ti_2C_2@C_{78}$ and $Ti_2S@C_{78}$. Titanium plays a special role in EMFs, since so far it is the only genuine transition metal that can be encapsulated inside the carbon cage. Two all-titanium EMFs characterized with a high degree of certainty are carbide $Ti_2C_2@C_{78}$[43–45] and sulfide $Ti_2S@C_{78}$,[46] both with $D_{3h}(5)$ carbon cage (mixed Ti–Sc[47] and Ti–Y[48] nitride clusterfullerenes are not considered here). Both EMFs have similar structures in that Ti atoms are η^6-coordinated to the poles of C_{78} (which has an elongated shape) and the Ti_2C_2 and Ti_2S

dx.doi.org/10.1021/ja4122582 | J. Am. Chem. Soc. 2014, 136, 4257–4264

clusters are almost linear (Figure 8a,b). Since Ti formally transfers three electrons to the carbon cage, pentalene is not

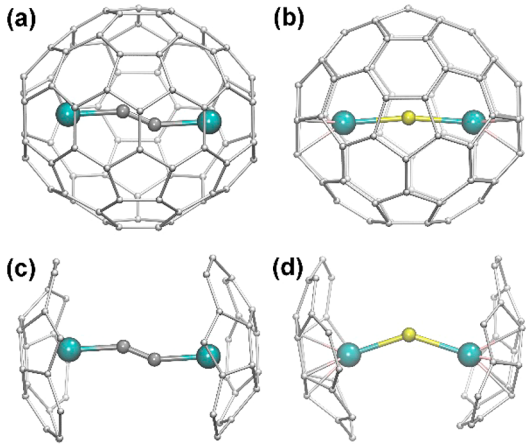

Figure 8. DFT-optimized molecular structures of (a) $Ti_2C_2@C_{78}$, (b) $Ti_2S@C_{78}$, (c) $Ti_2C_2(C_{21}H_9)_2$, and (d) $Ti_2S(C_{21}H_9)_2$. Ti atoms are shown in cyan, sulfur in yellow, and carbon atoms in gray. Hydrogen atoms in panels c and d are omitted for clarity.

able to mimic the metal−cage interactions and is replaced here by sumanene, $C_{21}H_9$ (Figure 8c,d).

DFT optimization of $Ti_2S(C_{21}H_9)_2$ results in a structure with bent Ti_2S cluster (Ti−S−Ti bond angle 143°), Ti−S bond length 2.328 Å, and Ti···Ti distance 4.417 Å. For comparison, in $Ti_2S@C_{78}$ these have the values 172° (Ti−S−Ti angle), 2.375 Å (Ti−S bond length), and 4.737 Å (Ti···Ti distance). Distortion energy of the Ti_2S cluster in $Ti_2S@C_{78}$ is estimated to be 10 kJ·mol^{-1}. Computation of the energy profile along cluster bending and Ti−S bond stretching shows that the Ti−S−Ti angle can vary in a relatively large range with modest energy increase (Figure 9a,b). The linear cluster is the energy maximum, but it is only 7 kJ·mol^{-1} less stable than the lowest energy configuration. Variation of Ti−S bond length shows that the energy remains below 10 kJ·mol^{-1} in the range 2.24−2.43

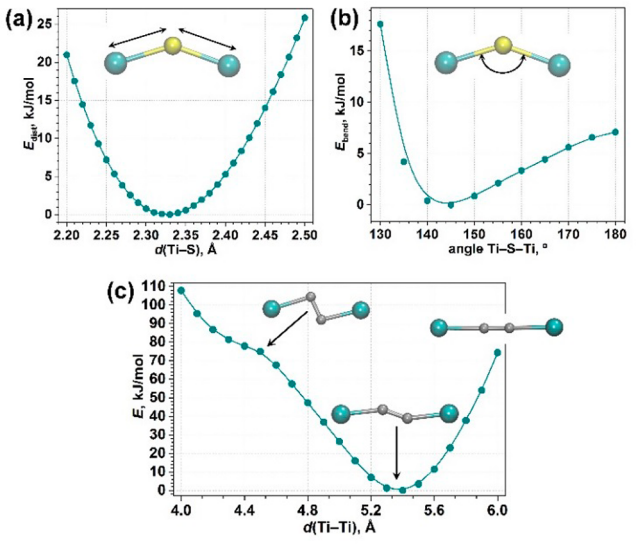

Figure 9. Energy profiles computed for (a) variation of Ti−S bond length in $Ti_2S(C_{21}H_9)_2$, (b) variation of Ti−S−Ti angle in $Ti_2S(C_{21}H_9)_2$, and (c) variation of Ti−Ti distance in $Ti_2C_2(C_{21}H_9)_2$.

Å. These results prove that the Ti_2S cluster is rather flexible, in similar fashion to Sc_2S and Y_2S clusters discussed above, and can change its shape over a rather broad range of geometrical parameters.

Unconstrained optimization of $Ti_2C_2(C_{21}H_9)_2$ shows that the Ti_2C_2 cluster prefers an almost linear configuration (Ti−C−C angle of 174.5°; see Figure 8c) with Ti···Ti distance of 5.377 Å (ca. 1 Å longer than in Ti_2S) and Ti−C bond length of 2.073 Å. In $Ti_2C_2@C_{78}$ Ti atoms are closer to each other (5.094 Å), Ti−C bonds are shorter (1.976 Å), and the cluster deviates more from linear shape (Ti−C−C angle is 154.2°). These structural changes increase the energy of the cluster by 26 kJ·mol^{-1}. Significant distortion energy shows that Ti_2C_2 cluster is more rigid than sulfide or Sc_2C_2 clusters, and the same conclusion can be drawn from analysis of the Ti···Ti energy profile (Figure 9c). In contrast to the flat Sc_2C_2 profile (Figure 6a), distortion energy of the Ti_2C_2 cluster remains below 10 kJ·mol^{-1} only in the 5.2−5.6 Å range and increases sharply outside these limits with either stretching or compression of the cluster. We could not find an energy minimum corresponding to the butterfly configuration down to the distances of 4.0 Å. The bend on the curve near 4.4 Å can be well seen, but the energy continues to increase at shorter Ti···Ti distances and exceeds 100 kJ·mol^{-1} at 4.0 Å. Thus, $Ti_2C_2@C_{78}$ is a real example of nanoscale fullerene compression.

Our analysis shows that although $Ti_2S@C_{78}$ and $Ti_2C_2@C_{78}$ are isostructural, they exhibit different kinds of cluster strain. For Ti_2S, the C_{78} cage appears to be too large, whereas for Ti_2C_2 it is too small, which in both cases results in nonnegligible distortion energy. Note that the effect is sufficient to induce measurable differences in geometrical parameters of the carbon cage. In $Ti_2C_2@C_{78}$ the distance between centroids of two Ti-coordinating hexagons (8.219 Å) is 0.176 Å longer than in $Ti_2S@C_{78}$ (8.045 Å). Likewise, Ti−hexagon distance in $Ti_2C_2@C_{78}$ (1.571 Å) is shorter than in $Ti_2S@C_{78}$ (1.659 Å). In other words, in $Ti_2C_2@C_{78}$ the cage is elongated and the Ti−C_6 distance is shortened to allow more space for the Ti_2C_2 cluster.

■ CONCLUSIONS

In this work we presented and evaluated a simple approach allowing analysis of the strain experienced by clusters encapsulated in endohedral metallofullerenes. We argue that calculations for the cluster alone, in either the neutral or charged state, cannot be used for this goal. However, when the effect of the carbon cage is mimicked by small organic π-systems (such as pentalene and sumanene), the cluster has sufficient freedom to adopt the optimal configuration, and therefore the energetic characteristics of EMF-induced distortion of the cluster can be evaluated. Both nitride and sulfide clusters were found to be rather flexible; that is, their distortion energy is small over a broad range of geometrical parameters. Hence, they can be encapsulated in carbon cages of different sizes and shapes. For carbide M_2C_2 cluster, the situation is more complex. The optimized cluster can adopt either butterfly or linear shapes, and these configurations have substantially different metal−metal distances. Whereas for Sc_2C_2 both structures are isoenergetic, the linear form of Y_2C_2 cluster is substantially less stable than the butterfly-shaped configuration. These results show that the phenomenon of nanoscale fullerene compression should be analyzed more carefully. Finally, we show that both Ti_2S and Ti_2C_2 clusters are strained in corresponding EMF molecules, but the origin of the

dx.doi.org/10.1021/ja4122582 | J. Am. Chem. Soc. 2014, 136, 4257−4264

strain is opposite: the C_{78}-$D_{3h}(5)$ cage imposes too-long Ti···Ti distance for the sulfide cluster and too-short distance for the carbide cluster.

■ ASSOCIATED CONTENT

Supporting Information

Additional text, three figures, and two tables with comparison of pentalene and *s*-indacene, computation of $[M_2C_2]^{4+}$ clusters, and correction of distortion energies due to interfragment interactions; additional tables with optimized atomic coordinates and energies. This material is available free of charge via the Internet at http://pubs.acs.org.

■ AUTHOR INFORMATION

Corresponding Author

a.popov@ifw-dresden.de

Notes

The authors declare no competing financial interest.

■ ACKNOWLEDGMENTS

This work was supported by DFG (Project PO 1602/1-1). Computational resources were provided by the Supercomputing Center of Moscow State University[49] and the Center for Information Services and High Performance Computing (ZIH) in TU-Dresden.

■ REFERENCES

(1) Stevenson, S.; Rice, G.; Glass, T.; Harich, K.; Cromer, F.; Jordan, M. R.; Craft, J.; Hadju, E.; Bible, R.; Olmstead, M. M.; Maitra, K.; Fisher, A. J.; Balch, A. L.; Dorn, H. C. *Nature* **1999**, *401*, 55.

(2) Popov, A. A.; Yang, S.; Dunsch, L. *Chem. Rev.* **2013**, *113*, 5989.

(3) Lu, X.; Feng, L.; Akasaka, T.; Nagase, S. *Chem. Soc. Rev.* **2012**, *41*, 7723.

(4) Rodriguez-Fortea, A.; Balch, A. L.; Poblet, J. M. *Chem. Soc. Rev.* **2011**, *40*, 3551.

(5) Chaur, M. N.; Melin, F.; Ortiz, A. L.; Echegoyen, L. *Angew. Chem., Int. Ed.* **2009**, *48*, 7514.

(6) Yang, S.; Liu, F.; Chen, C.; Jiao, M.; Wei, T. *Chem. Commun.* **2011**, *47*, 11822.

(7) Dunsch, L.; Yang, S. *Small* **2007**, *3*, 1298.

(8) Zhang, J.; Stevenson, S.; Dorn, H. C. *Acc. Chem. Res.* **2013**, *46*, 1548.

(9) Wang, C. R.; Kai, T.; Tomiyama, T.; Yoshida, T.; Kobayashi, Y.; Nishibori, E.; Takata, M.; Sakata, M.; Shinohara, H. *Angew. Chem., Int. Ed.* **2001**, *40*, 397.

(10) Lu, X.; Akasaka, T.; Nagase, S. *Acc. Chem. Res.* **2013**, *46*, 1627.

(11) Jin, P.; Tang, C.; Chen, Z. *Coord. Chem. Rev.* **2013**, DOI: 10.1016/j.ccr.2013.10.020.

(12) Dunsch, L.; Yang, S.; Zhang, L.; Svitova, A.; Oswald, S.; Popov, A. A. *J. Am. Chem. Soc.* **2010**, *132*, 5413.

(13) Chen, N.; Chaur, M. N.; Moore, C.; Pinzon, J. R.; Valencia, R.; Rodriguez-Fortea, A.; Poblet, J. M.; Echegoyen, L. *Chem. Commun.* **2010**, *46*, 4818.

(14) Popov, A. A.; Dunsch, L. *J. Am. Chem. Soc.* **2007**, *129*, 11835.

(15) Rodriguez-Fortea, A.; Alegret, N.; Balch, A. L.; Poblet, J. M. *Nat. Chem.* **2010**, *2*, 955.

(16) Kobayashi, K.; Nagase, S.; Akasaka, T. *Chem. Phys. Lett.* **1995**, *245*, 230.

(17) Popov, A. A. *J. Comput. Theor. Nanosci.* **2009**, *6*, 292.

(18) Yang, S. F.; Popov, A. A.; Dunsch, L. *Angew. Chem., Int. Ed.* **2007**, *46*, 1256.

(19) Popov, A. A.; Krause, M.; Yang, S. F.; Wong, J.; Dunsch, L. *J. Phys. Chem. B* **2007**, *111*, 3363.

(20) Chen, N.; Mulet-Gas, M.; Li, Y.-Y.; Stene, R. E.; Atherton, C. W.; Rodriguez-Fortea, A.; Poblet, J. M.; Echegoyen, L. *Chem. Sci.* **2013**, *4*, 180.

(21) Olmstead, M. M.; de Bettencourt-Dias, A.; Duchamp, J. C.; Stevenson, S.; Marciu, D.; Dorn, H. C.; Balch, A. L. *Angew. Chem., Int. Ed.* **2001**, *40*, 1223.

(22) Zhang, J.; Fuhrer, T.; Fu, W.; Ge, J.; Bearden, D. W.; Dallas, J. L.; Duchamp, J. C.; Walker, K. L.; Champion, H.; Azurmendi, H. F.; Harich, K.; Dorn, H. C. *J. Am. Chem. Soc.* **2012**, *134*, 8487.

(23) Popov, A. A.; Dunsch, L. *Chem.—Eur. J.* **2009**, *15*, 9707.

(24) Perdew, J. P.; Burke, K.; Ernzerhof, M. *Phys. Rev. Lett.* **1996**, *77*, 3865.

(25) Laikov, D. N.; Ustynuk, Y. A. *Russ. Chem. Bull.* **2005**, *54*, 820.

(26) Laikov, D. N. *Chem. Phys. Lett.* **2005**, *416*, 116.

(27) Laikov, D. N. *Chem. Phys. Lett.* **1997**, *281*, 151.

(28) Humphrey, W.; Dalke, A.; Schulten, K. *J. Mol. Graphics* **1996**, *14*, 33.

(29) Chen, N.; Beavers, C. M.; Mulet-Gas, M.; Rodriguez-Fortea, A.; Munoz, E. J.; Li, Y.-Y.; Olmstead, M. M.; Balch, A. L.; Poblet, J. M.; Echegoyen, L. *J. Am. Chem. Soc.* **2012**, *134*, 7851.

(30) Mercado, B. Q.; Chen, N.; Rodriguez-Fortea, A.; Mackey, M. A.; Stevenson, S.; Echegoyen, L.; Poblet, J. M.; Olmstead, M. M.; Balch, A. L. *J. Am. Chem. Soc.* **2011**, *133*, 6752.

(31) Kurihara, H.; Lu, X.; Iiduka, Y.; Nikawa, H.; Hachiya, M.; Mizorogi, N.; Slanina, Z.; Tsuchiya, T.; Nagase, S.; Akasaka, T. *Inorg. Chem.* **2012**, *51*, 746.

(32) Krause, M.; Hulman, M.; Kuzmany, H.; Dubay, O.; Kresse, G.; Vietze, K.; Seifert, G.; Wang, C.; Shinohara, H. *Phys. Rev. Lett.* **2004**, *93*, 137403.

(33) Feng, Y.; Wang, T.; Wu, J.; Feng, L.; Xiang, J.; Ma, Y.; Zhang, Z.; Jiang, L.; Shu, C.; Wang, C. *Nanoscale* **2013**, *5*, 6704.

(34) Kurihara, H.; Lu, X.; Iiduka, Y.; Mizorogi, N.; Slanina, Z.; Tsuchiya, T.; Akasaka, T.; Nagase, S. *J. Am. Chem. Soc.* **2011**, *133*, 2382.

(35) Iiduka, Y.; Wakahara, T.; Nakajima, K.; Tsuchiya, T.; Nakahodo, T.; Maeda, Y.; Akasaka, T.; Mizorogi, N.; Nagase, S. *Chem. Commun.* **2006**, 2057.

(36) Nishimoto, Y.; Wang, Z.; Morokuma, K.; Irle, S. *Phys. Status Solidi B* **2011**, *249*, 324.

(37) Inoue, T.; Tomiyama, T.; Sugai, T.; Shinohara, H. *Chem. Phys. Lett.* **2003**, *382*, 226.

(38) Zhang, J.; Bowles, F. L.; Bearden, D. W.; Ray, W. K.; Fuhrer, T.; Ye, Y.; Dixon, C.; Harich, K.; Helm, R. F.; Olmstead, M. M.; Balch, A. L.; Dorn, H. C. *Nat. Chem.* **2013**, *5*, 880.

(39) Yang, T.; Zhao, X.; Li, S.-T.; Nagase, S. *Inorg. Chem.* **2012**, *51*, 11223.

(40) Yang, H.; Jin, H.; Hong, B.; Liu, Z.; Beavers, C. M.; Zhen, H.; Wang, Z.; Mercado, B. Q.; Olmstead, M. M.; Balch, A. L. *J. Am. Chem. Soc.* **2011**, *133*, 16911.

(41) Burke, B. G.; Chan, J.; Williams, K. A.; Fuhrer, T.; Fu, W.; Dorn, H. C.; Puretzky, A. A.; Geohegan, D. B. *Phys. Rev. B* **2011**, *83*, No. 115457.

(42) Yang, H.; Lu, C.; Liu, Z.; Jin, H.; Che, Y.; Olmstead, M. M.; Balch, A. L. *J. Am. Chem. Soc.* **2008**, *130*, 17296.

(43) Cao, B. P.; Hasegawa, M.; Okada, K.; Tomiyama, T.; Okazaki, T.; Suenaga, K.; Shinohara, H. *J. Am. Chem. Soc.* **2001**, *123*, 9679.

(44) Yumura, T.; Sato, Y.; Suenaga, K.; Iijima, S. *J. Phys. Chem. B* **2005**, *109*, 20251.

(45) Tan, K.; Lu, X. *Chem. Commun.* **2005**, 4444.

(46) Li, F.-F.; Chen, N.; Mulet-Gas, M.; Triana, V.; Murillo, J.; Rodriguez-Fortea, A.; Poblet, J. M.; Echegoyen, L. *Chem. Sci.* **2013**, *4*, 3404.

(47) Yang, S.; Chen, C.; Popov, A.; Zhang, W.; Liu, F.; Dunsch, L. *Chem. Commun.* **2009**, 6391.

(48) Chen, C.; Liu, F.; Li, S.; Wang, N.; Popov, A. A.; Jiao, M.; Wei, T.; Li, Q.; Dunsch, L.; Yang, S. *Inorg. Chem.* **2012**, *51*, 3039.

(49) Voevodin, V. V.; Zhumatiy, S. A.; Sobolev, S. I.; Antonov, A. S.; Bryzgalov, P. A.; Nikitenko, D. A.; Stefanov, K. S.; Voevodin, V. V. *Open Syst. J.* **2012** (7), http://www.osp.ru/os/2012/07/13017641/.